Identifying Biomarkers for Evaluating Wound Extent and Age in the Contused Muscle of Rats Using Microarray Analysis: A Pilot Study

Na Li[1], Chun Li[1], Dan Li[1], Li-hong Dang[1], Kang Ren[1], Qiu-xiang Du[1], Jie Cao[1], Qian-qian Jin[1], Ying-yuan Wang[1], Ru-feng Bai[2]* and Jun-hong Sun[1]*

[1] School of Forensic Medicine, Shanxi Medical University, Jinzhong 030604, Shanxi, China;
[2] Key Laboratory of Evidence Science, China University of Political Science and law, Beijing, China; Collaborative Innovation Center of Judicial Civilization, Beijing, China

Corresponding Author:
Jun-hong Sun[1]
98 University Street, Yuci District, Jinzhong 030604, Shanxi, People's Republic of China.
Email address: junhong.sun@sxmu.edu.cn
Ru-feng Bai[2]
Chinese University of Political Science and Law, Beijing 100040, People's Republic of China
Email address: bairufeng@cupl.edu.cn

Abstract

Wound age estimation is still one of the most important and significant challenges in forensic practice. The extent of wound damage greatly affects the accuracy and reliability of wound age estimation, so it is important to find effective biomarkers to help diagnose wound degree and wound age. In the present study, the gene expression profiles of both mild and severe injuries in 33 rats were assayed at 0, 1, 3, 24, 48, and 168 hours using the Affymetrix microarray system to provide biomarkers for the evaluation of wound age and the extent of the wound. After obtaining thousands of differentially expressed genes, a principal component analysis, the least absolute shrinkage and selection operator, and a time-series analysis were used to select the most predictive prognostic genes. Finally, fifteen genes were screened for evaluating the extent of wound damage, and the top 60 genes were also screened for wound age estimation in mild and severe injury. Selected indicators showed good diagnostic performance for identifying the extent of the wound and wound age in a Fisher discriminant analysis. A function analysis showed that the candidate genes were mainly related to cell proliferation and the inflammatory response, primarily IL-17 and the Hematopoietic cell lineage signalling pathway. The results revealed that

35 these genes play an essential role in wound-healing and yield helpful and valuable potential

36 biomarkers for further targeted studies.

Introduction

38 In violent cases, an accurate estimation of wound age, which describes the time interval between

39 trauma infliction and death, is one of the most challenging points in forensic pathology *(Casse et*

40 *al. 2016; Trautz et al. 2019; Wang et al. 2016)*. The precise estimation of wound age contributes

41 to rebuilding the scene of the case, demarcating the scope of suspects, determining the nature of

42 the cases, and finally facilitating the investigation process *(Du et al. 2020; Sun et al. 2017)*.

43 However, the determination of wound age is influenced by many additional factors such as age,

44 gender, concomitant diseases, therapy, and the extent of the wound damage making it even

45 harder to ensure the accuracy and reliability of wound age prediction *(Grellner & Madea 2007;*

46 *Li et al. 2018)*. Among these factors, the extent of a wound, which is highly variable among the

47 muscles examined in forensic practice, may be the most important.

48   It is well known that wound age estimation mainly depends on the time-dependent

49 expression patterns of the molecules involved in damage repair. Although skeletal muscle holds

50 an innate capacity for self-repair after injury, fibrosis, or fatty muscle deposits with significant

51 functional deficits, often occur in the case of severe injury. Fibrosis is related to both the

52 different molecular responses after injury as well as the severity of the wound. Thus, the

53 temporal expression pattern of molecules responding to injury varies with both the stage of the

54 healing process and the severity of the injury. Most studies have concentrated solely on the

55 timing of morphological and biochemical changes during wound healing *(Hassan Gaballah et al.*

56 *2016; Ishida et al. 2015; Wang et al. 2015)* and have ignored the effect of the level of wound

57 damage. A careful evaluation of the extent of a wound is necessary to effectively determine

58 wound age.

59   With the rapid development of life science and technology, particularly high-throughput

60 technology, the measurement of damage parameters has improved, and more and more potential

61 biomarkers for estimating the time of injury have been studied *(Casse et al. 2016; Li et al. 2018)*.

62 Microarray technology, which allows the simultaneous evaluation of the expression profiles of

63 thousands of genes, has increasingly contributed to our understanding of many biological

64 processes *(Komamura et al. 2003; Li et al. 2017)* and also shows great potential for identifying

65 valuable biomarkers of the time-dependent expression for wound age estimation. The main

66 problem with using microarray technology is that the number of genes greatly exceeds the

67 number of samples following a microarray experiment, leading to the main concern of how to

68 identify genes of interest from such a large gene set.

69 Fortunately, the least absolute shrinkage and selection operator (LASSO) regression model

70 was introduced with the potential to solve this problem. In a LASSO-penalized regression, as log

71 λ (a tuning parameter) changes, the corresponding coefficients of certain genes are reduced to

72 zero, indicating that their effects on the model can be omitted because they are shrunk

73 parameters *(Tibshirani 1997)*. LASSO regressions allow fewer hub genes to be obtained for

74 further analysis. Moreover, a time-series analysis, based on the multivariate empirical Bayes'

75 statistic (MBstatistic), is sufficient to find genes with large differences in their temporal patterns

76 between conditions and then rank them *(Tai & Speed 2009)*. We applied the LASSO method in

77 our study to evaluate the most informative prognostic mRNA biomarkers according to their

78 relative contribution to the prognosis of damage degree; we also used a time-series analysis to

79 identify genes with large differences in temporal profiles for wound aging.

80 In a previous study, we established the muscle contusion models of rats caused by blunt

81 force attack at different heights, and evaluated the gross and histological morphological changes

82 over time as well as verified the repeatability of the model *(Bai et al. 2017)*. Different numbers

83 of inflammatory cells and different sizes of hemorrhage and edema were observed in mild and

84 severe contusion muscles. In this study, we aimed to explore the molecular changes at the

85 transcriptional level of mildly and severely contused muscle and identify valuable potential

86 biomarkers for evaluating the extent of the wound as well as wound age. Because basic

87 physiological responses are similar in both humans and animals, the predictive genes for wounds

88 found in this study will provide valuable information for further forensic practice.

Materials & Methods

Animal model and tissue preparation

91 All procedures were performed according to the "Guiding Principles in the Use and Care of

92 Animals" (NIH Publication No. 85-23, Revised 1996) and were approved by the Institutional

93 Animal Care and Use Committee of Shanxi Medical University of China [Batch number of rats:

94 SCXK (Jin) (2009-0001)]. Animals received humane care in conformity to the principles in the

95 Guide for the Care and Use of Laboratory Animals protocol, published by the Ministry of the

96 People's Republic of China (issued on June 4, 2004). The laboratory personnel were given

97   permission to conduct this study by the Committee after they attended and completed training on

98   how to use experimental animals ethically. All male Sprague Dawley rats were purchased from

99   the Animal Center of Shanxi Medical University. This study was carried out in compliance with

100   the ARRIVE guidelines and evaluated and approved by the Institutional Animal Care and Use

101   Committee of Shanxi Medical University of China with approval number 2019sll002.

102   An animal model was established based on previous studies *(Bai et al. 2017)*. In total, 33

103   male Sprague Dawley rats (aged 10-12 weeks), weighing 250-300g, were placed in a cage with

104   rat chow and water, under a 12-hour light-dark cycle in a temperature-controlled room (22-24℃)

105   with a relative humidity of 40-60%. No adverse events were observed. All rats were randomly

106   divided into three groups:

107   (1) Control group (n=3): without any treatment before sampling.

108   (2) Mild contusion groups (n=15): a 500g counterpoise fell freely from a height of 15 cm

109   down a clear Lucite guide tube onto the thigh muscles of the right posterior limb with the

110   potential energy of the contusion totaling about 1.46 J/cm^2 (the formula: Ep=mgh).

111   (3) Severe contusion groups (n=15): a 500g counterpoise fell freely from a height of 50 cm,

112   with the potential energy of contusion at about 2.58J/cm^2 (the formula: Ep=mgh).

113   The animals in the mild and severely contused groups were further divided into five

114   subgroups (1-, 3-, 24-, 48-, and 168-hour post-injury; n=3/subgroup) for microarray analysis.

115   Before muscle contusion, the rats were anesthetized with pentobarbital sodium to minimize the

116   suffering of the rats during the experimental period. The rats in the contusion groups were

117   sacrificed at the above timepoints with a lethal dose of pentobarbital (350 mg/kg body weight,

118   intraperitoneal injection). Approximately 100 mg of muscle was sampled from the wound site

119   and equally divided into two parts from each rat. For the control rats, specimens were harvested

120   from the same site after anesthetization with a lethal dose of pentobarbital. All the muscle

121   samples from 33 rats were frozen immediately with liquid nitrogen for the microarray analysis.

122   A further 56 rats were randomly allocated to a control group (n=8) and 4-, 8-, 12-, 16-, 20-,

123   24-, 28-, 32-, 36-, 40-, 44-, and 48-h (n=6/group) mild contusion groups for qPCR. Before

124   contused, the right posterior limbs of the rats with pentobarbital were shaved by a depilatory

125   agent (Nair; Carter Wallace, New York, NY, USA) and placed on an experimental table in a

126   supine position. After damage, the rats were transferred into clean cages with food and water.

RNA extraction

Total RNA was extracted as described in previous study *(Du et al. 2020)*. Specifically, we isolated the RNA from the skeletal muscle specimens (approximately 50 mg each) using RNAiso Plus 9108 (Takara Bio, Shiga, Japan), according to the manufacturer's protocol. The quantity (ng/mL) and purity of RNA were accessed by a microplate reader (Infinite M200 Pro; TECAN, Zurich, Switzerland), and the integrity of the RNA was further analyzed with an Agilent 2100 instrument (Agilent Technologies, Palo Alto, CA, USA) using an Agilent RNA 6000 Nano kit. Only RNAs with OD260/OD280 ratios ranging from 1.8 to 2.2 and a RIN > 7.0 were selected for the microarray and the RT-PCR (reverse transcription polymerase chain reaction).

Microarray analysis

Total RNA was used to synthesize sense-strand cDNA (sscDNA) using the Ambion WT Expression Kit. Then, fragmentated and labeled sscDNA samples (using the Affymetrix® GeneChip® WT Terminal Labeling Kit) were hybridized to Gene 1.1 ST Array Plates. Washed and stained arrays were scanned using the GeneChip Scanner 3000 7G.

Data processing

Statistical significance of gene expression differences between the contusion and control groups was analyzed using one-way ANOVA in the Affymetrix Transcriptome Analysis Console software version 4.0.1. The expressions of mRNA with fold change >2 in mean expression compared with the control group and a P-value of <0.05 and FDR (false discovery rate) <0.05 were considered differentially expressed genes (DEGs).

A heatmap and an unsupervised hierarchical clustering analysis were performed to cluster DEGs in the mild and severe groups, respectively, using the online software Morpheus (https://software.broadinstitute.org/morpheus). Principal component analysis (PCA) was employed to evaluate the importance of DEGs, distinguish the extent of contusions, and visualize the effect of the DEGs we selected in wound age estimation based on different wound degrees using SIMC A-P (ver. 14.1; Umetrics, Malmö, Sweden). T-distributed Stochastic Neighbor Embedding (t-SNE) was performed by R package "tsne" (version 0.15).

A least absolute shrinkage and selection operator (LASSO) regression model was then used to select key genes through a penalized likelihood approach *(Tibshirani 1997)*. In the model, as log λ (a tuning parameter) changed, the regression coefficients penalize the size of the parameters, so that the coefficient estimates of unimportant variables can shrink towards

158   zero*(Yan et al. 2020)*. Moreover, the "time course" R package was applied to find genes of

159   interest based on the multivariate empirical Bayes model. It was reported that this model was

160   superior to the traditional F-statistic for the analysis of time-series data *(Tai & Speed 2009)*.

161   Gene ontology (GO) annotation was conducted using the Gene Ontology Consortium

162   (http://geneontology.org) and the Kyoto encyclopedia of genes and genomes (KEGG) pathway

163   annotation was performed by clueGo plugin (https://apps.cytoscape.org/apps/cluego) *(Bindea et*

164   *al. 2009)*. The protein-protein interaction (PPI) network was built by STRING 11.0

165   (https://string-db.org) and the networks were visualized and exported from Cytoscape 3.7.2

166   *(Shannon et al. 2003)*. In addition, the top 10 hub genes in the PPI network were selected

167   according to the degree method using the plug-in CytoHubba in Cytoscape *(Chin et al. 2014)*. A

168   Fisher discriminant analysis (FDA) was performed using SPSS software (SPSS version 24.0)

169   **Quantitative real-time PCR**

170   We prepared the reaction mixtures using the Premix Ex Taq ™ kit (Takara Biotechnology Co.,

171   Ltd., Dalian, China) and then put them into the Bio-Rad CFX384 fluorescence Quantitative PCR

172   system (CFX384; Bio-Rad, Hercules, CA, USA) . Amplification was performed using a 2-step

173   cycling program according to the following conditions:40 cycles of 5 seconds at 95 °C, 40

174   seconds at 58–60 °C. Two reference (RPL13, ribosomal protein L13; RPL32, ribosomal protein

175   L32) and two target genes were simultaneously assayed, as they were in previous studies *(Dang*

176   *et al. 2020; Du et al. 2020)*. Each reaction mixture consisted of Taq DNA polymerase (12.5 μL),

177   upstream and downstream primers and probes (0.65 μL; eight primers and four probes), 10%

178   (v/v) DMSO (2.0 μL), deionized water (1.2 μL), and cDNA (1.5 μL). The primers and probes

179   that were used are listed in Table S1.

180   The flow diagrams, shown in Figure 1, summarize the experimental and data analysis procedures

181   used in the present study.

182   **Results**

183   **Transcriptional profiles in mildly and severely contused muscle**

184   After ruling out probes with low expressions, 16,005 probes were selected from 33 rats for the

185   next analysis. There were 2,843 DGEs presented in the mild contusion groups and 2,298 DEGs

186   in the severe contusion groups compared with the control group (Fig.2a, d). The number of

187   DGEs found in mild injury was larger than that found in severe injury except at 168 hours. And

188   at each time point, compared with the control group, the number of upregulated DGEs was more

189 than down-regulated even with different degrees of injury (Fig.2b,2c). A PCA analysis of unique

190 genes showed that the mildly and severely contused groups were clearly separated from each

191 other, indicating that the severity of damage contributes the most to the variance in the data set

192 (Fig.2e).

193 **Hub genes to distinguish the extent of the injury**

194 The unique DEGs expressed between the mild and severe damage groups were then used to

195 assess the extent of wound damage. In a principal component analysis of unique genes, over 70%

196 of the variance among the DEGs was retained in the first five principal components (PCs)

197 (Fig.3a). The score of each principal component is displayed in Fig.3b-c and Fig.1S.a-c.

198 Although the variance of the first principal component (PC1) was the largest of the first five

199 principal components, PC2 captured most of the variance related to the genes expressed between

200 the mild and severe groups (Fig.3a-c). As in Fig.3c, the mild and severe contusion groups were

201 distributed in different areas on PC2, so the top 200 leading genes in PC2 were selected for

202 further analysis.

203 A least absolute shrinkage and selection operator (LASSO) regression model was then used

204 to select key genes *(Tibshirani 1997)*. We conducted the LASSO algorithm with the R "glmnet"

205 package *(Friedman et al. 2010)*, and the optimal tuning parameter (λ) was chosen to achieve the

206 minimal partial likelihood deviance in the cross-validation plot (Fig.1S d-e). The fifteen genes

207 with non-zero corresponding coefficients were entered into the multivariate model (Table S2).

208 The PCA score plots showed that the control group and the mild and severe contusion groups

209 were clearly separated from each other, indicating that the expression of 15 genes differed in

210 mildly and severely contused muscle (Fig.3d). This conclusion was also supported by a random

211 forest analysis (Fig.3e).

212 **The screening of candidate markers for injury time estimation in mild contusion**

213 Candidate markers with time-series analysis

214 An unsupervised hierarchical clustering analysis of 2843 DEGs in the mild contusion groups

215 showed that the expression profiles of mild injury at the six observed time points could be

216 segregated into three distinct clusters: the first cluster included contused muscle 24 and 48 hours

217 after injury; the second cluster included contused muscle 0, 1, and 168 hours post-injury; and the

218 third cluster included contused muscle 3 hours after injury (Fig.4a). PCA of all DEGs in mild

219 injury also showed that the samples displayed a temporal separation in the PCA space (Fig.4b).

220   One sample at 1h that was clustered with the 3h samples may be related to the fact that 1h and 3h

221   are very close and hierarchical clustering and PCA are unsupervised analyses with limited

222   discriminating ability. In addition, the fact that the samples of 1h were grouped with 168h may

223   be due to the similarity between the beginning and the end of the inflammation stage as both had

224   a few DEGs with similar expression profiles. Generally, the transcriptome profiles exhibited

225   time-dependent patterns that allowed us to identify useful markers of wound age.

226   For wound aging, the "time course" package in R language was used to obtain genes with

227   large differences in their temporal patterns over time after injury based on the empirical Bayes

228   model. Finally, the top 60 genes were chosen as candidate genes by their HotellingT2 value in

229   descending order (Table S3). The top 3 genes with different expression profiles in mild injury

230   were visualized and displayed in Fig.4c-e. A heatmap for the top 60 DEGs revealed that these

231   genes were expressed in four different temporal patterns, and the gene expression in these four

232   clusters were significantly increased over the period after injury (Fig.4f). Moreover, a t-SNE

233   analysis of these 60 DEGs showed different distributions for different contusion groups and that

234   they had the predictive potential for wound estimation in mild contusion groups (Fig.4g).

235   Bioinformatics analysis of candidate markers

236   To associate the changes of gene expressions with biological functions in mild injury, we

237   conducted a GO enrichment analysis of the top 60 genes to determine the enriched GO terms.

238   DEGs were categorized by their function into biological processes, cellular component, and

239   molecular function. $P < 0.05$ was used as a threshold to select significant GO categories in the

240   Gene Ontology Consortium and for KEGG pathway analysis in clueGo plugin (Fig.5a,5b). In

241   mild injury groups, we found that the top 3 categories of biological processes were related to

242   interspecies interaction between organisms, inflammatory response, and response to an external

243   stimulus. GO categories of cellular components were associated with myofibril, contractile fiber,

244   and sarcomere, and those related to molecular functions were relevant to cytokine activity,

245   signaling receptor activator activity, and receptor-ligand activity, suggesting the importance of

246   these genes during mild injury estimation. To identify the functional relationship among genes, a

247   PPI network of 60 genes was created and all genes had a STRING score of 0.7 or greater. We

248   used cytoHubba in Cytoscape to determine the hub genes, all of which play critical regulatory

249   roles in the PPI network. The top 15 genes with a high degree of connectivity were: Il1b, Il6,

250   Ccl2, Il18, Cxcl2, Timp1, Serpine1, Hmox1, Cxcr2, Cxcl6, Mmp8, Ccl7, Spp1, Ccr1 and Tnni1,

251   which were on the inside of the circle (Fig.5c).

252   **The screening of candidate markers for severe injury time estimation**

253   Candidate markers with time-series analysis

254   For expression profiling of the severely contused group, we used the same methods as in the

255   mildly contused groups. The PCA and unsupervised hierarchical clustering analysis of 2298

256   DEGs in the severe contusion groups revealed that samples from each time point were clustered

257   into a single group. Cluster analysis indicated two distinct transcriptome patterns of mild injury

258   in a time-dependent manner, which was supported by PCA results (Fig.6a, 6b). The empirical

259   Bayes model was also conducted using the 'time course' R package to rank genes based on their

260   expression over time. Lastly, the top 60 genes were acquired by their HotellingT2 values in

261   descending order for wound age estimation in severe contusion (Table S4). The top 3 genes with

262   different expression profiles in severe injury were visualized and displayed in Fig.6c-e. A

263   heatmap for the top 60 DEGs revealed that the majority of genes were highly expressed in the

264   late stage of injury (Fig.6f). Additionally, a t-SNE analysis of these 60 DEGs showed a

265   separation among the contused groups, revealing that their expression differed over time and

266   deserved to be explored further for wound age estimation (Fig.6g).

267   Bioinformatics analysis of candidate markers

268   In severely contused muscle, the top 3 categories of biological processes were related to defense

269   response, interspecies interaction between organisms, and response to external biotic stimulus.

270   Those of cellular components were associated with the external side of the plasma membrane,

271   and those of molecule functions were relevant to signaling receptor binding, cytokine activity,

272   and signaling receptor activator activity (Fig.7a). A KEGG analysis of the top 60 genes in the

273   clueGo plugin revealed that there were common pathways in both mild and severe injury

274   estimation such as the IL-17 signaling pathway and Hematopoietic cell lineage as well as unique

275   pathways in mild injury estimation including cytokine-cytokine receptor interaction and the TNF

276   signaling pathway (Fig.7b,7b). Most of these pathways were related to the process of injury and

277   repair, in which genes regulated the process of inflammation, for example, Cxc16, Ccr1, Csf3r,

278   Cxcr2, Il18, Cc17, Cc12, Il6, and Cxc12. Moreover, some pathways associated with bacterial

279   infection appeared such as Malaria and Salmonella infection, which may have close associations

280   with the inflammatory response. Using the STRING platform, the PPI network was built of these

281   60 genes in severe injury with a STRING score ≥0.7. The top 15 hub genes determined by

282   cytoHubba were: Cd68, Il6, Ptprc, Tyrobp, Ccl2, Csf1r, C3ar1, Cybb, Fcgr1a, Cd53, Lgals3,

283   Timp1, Spp1, Tlr7, and Cd163 (Fig.7c).

284   **Validation of markers in mild injury by quantitative real-time PCR**

285   We validated the microarray data by examining the expression of Mt2a, Rrad, Gpnmb, and Timp1 (shared

286   genes of selected top60 genes of mild and serve injury) in the mild contusion groups using RT-qPCR

287   (Fig.8e-h). In previous studies, we verified the time-dependent expression of Mt2a mRNA in the contused

288   skeletal muscle of rats within 36 hours by RT-qPCR *(Fan et al. 2017)* (Fig.8e). Ling et al *(Ling et al.*

289   *2016)* found that Mt2a is closely associated with oxidative stress, mediated by subcellular pathways of

290   mitochondria, ER, lysosomal, and lipidosome, as well as the MAPKs (ERK, JNK, and p38) signal. In

291   present study, we continued to validate the expression of Rrad, Gpnmb, and Timp1(Fig.7f-h, Table S5) in

292   56 rats. The expressions of Mt2a, Gpnmb, and Timp1 detected by RT-qPCR were elevated in a time

293   course manner, which was consistent with the results of the microarray (Fig.8a-d). Although the profiles

294   of Rrad were not identical to what we obtained from the microarray, mRNA of Rrad was upregulated

295   within 24h compared with the control group and corresponded to the Affymetrix analyses. Collectively,

296   the consistency between the results of qPCR and the microarray analyses confirmed the reproducibility of

297   the microarray data.

298   **Performance of screened genes in Fisher discriminant analysis**

299   To validate the predictive and diagnostic performance of selected indicators, a Fisher

300   discriminant analysis (FDA) was employed. Based on the expression of fifteen hub genes, the

301   canonical functions can differentiate between the control, mild, and severe groups (Fig.9a). The

302   classification results showed 90.9% accuracy for cross-validated grouped cases (seen in Table

303   S6), indicating that the molecules may respond differently during the repair process of mild and

304   severe injuries. For wound age estimation in mild injury, Lgmn, PVR, Hmox1, Egr1, Socs3,

305   Ankrd1, Cd8a, Pfkfb1, Msr1, Tnni1, and Myl3 of the top 60 candidate genes showed good

306   performance with only one wrongly classified sample of 168h n model of FDA (Fig.9b). In

307   severe injury, Apoe, Hmox1, Clec4a1, Egr1, Rrad, Il1rn, Akr1b8, C3ar1, Pltp, Ly49si1, and

308   Lilrb4 of the top 60 genes were included in the FDA model using the stepwise method and the

309   Wilks' lambda option. The results showed that all the samples were classified correctly (Fig.9c,

310   Table S7-8). Collectively, the fifteen hub genes and 120 candidate genes we provided showed

311   great potential for determining the extent of the wound and wound age and are valuable

312   candidates for further study.

Discussion

313

314 Although a number of research projects have investigated how to determine the time of injuries,

315 significant barriers remain in the application of useful biomarkers to establish the chronology of

316 an injury in forensic practice. There are many factors that contribute to wound age estimation,

317 but one factor that plays as essential role in wound age estimates is the extent of the wound.

318 However, most studies focus on the changes at the morphological and molecular levels in bruises

319 over time without considering the impact of the force used to inflict the trauma. Barington K et

320 al. *(Barington & Jensen 2016)* made an attempt to compare the changes of bruises inflicted with

321 a low, moderate, and high force, but they only explored bruises within 8h at gross and

322 histological levels which is still far from practical applications.

323   In cases of violent injury, the severity of muscle bruising often varies among individuals

324 and among sites of damage within the same individual. Forensic pathologists mostly estimate

325 wound age based on the time-dependent changes of the molecules' response to an injury and the

326 morphological transformation caused by these molecules *(Dang et al. 2020; Wang et al. 2016)*.

327 Many wound healing-related biomarkers have recently been explored for wound aging *(Hassan*

328 *Gaballah et al. 2016; Ishida et al. 2018; Kubo et al. 2014)*; however, only a few markers have

329 sufficient diagnostic power for high-accuracy wound age estimation, which is partly because the

330 molecules respond differently at different levels of damage.

331   Therefore, it is important to identify useful biomarkers to evaluate the extent of a wound

332 and then to determine injury time. In this study, experimental animal models of muscle contusion

333 with different heights of blunt force were developed, and microarray technology was utilized to

334 identify a series of markers over time at the transcriptome level. Our study aimed to screen

335 useful markers to evaluate the extent of a wound, estimate damage time, and to be used for

336 further studies of wound age.

337   We first identified a total of 3,522 DEGs in mildly and severely contused muscle compared

338 to normal skeletal muscle in rats. According to PCA results, we found that unique genes can

339 better distinguish mild and severe injury than the genes that are shared between the two groups.

340 In order to discover indicators that contribute more to the discrimination of damage degrees, the

341 top 200 leading genes in PC2 of five principal components were chosen for subsequent analysis

342 (Fig.2c). In order to select the most powerful predictive prognostic genes for identifying the

343 extent of the wound damage, the least absolute shrinkage and selection operator (LASSO)

344   regression model was used for variable shrinkage. Finally, 15 key genes were selected. The PCA

345   score plots showed that the control group and the mild and severe contusion groups were clearly

346   separate from each other, indicating that the expression of the 15 key genes differed in mildly

347   and severely contused muscle (Fig.3d-e). This conclusion was also supported by a random forest

348   analysis.

349   In addition, most of these 15 genes have been previously reported to play a vital role in cell

350   proliferation and the inflammatory response. Reducing APIP expression could help treat

351   systemic inflammatory response syndrome, a whole-body inflammatory state that can occur in

352   response to infection *(Ko et al. 2012)*. Fam220a genes have been identified as novel target genes

353   for miR-489-3p and miR-92a-3p associated with renal injury and hypercholesterolemia *(Wiese et*

354   *al. 2019)*. Myadml2, which encodes myeloid-associated differentiation marker-like 2, may

355   influence the ability of dairy cows to resist the inflammation response of mastitis *(Chen et al.*

356   *2015)*. Trim72, with a RING finger domain, a B-box, two coiled-coil domains, and a SPRY

357   domain, is specifically expressed in the plasma membrane of skeletal and cardiac muscle cells

358   and is transcriptionally activated by the synergism of MyoD (or myogenin) and MEF2 *(Cai et al.*

359   *2009; Jung & Ko 2010; Lee et al. 2010)*. Ntn1, which encodes netrin 1, is a target of the

360   Wnt/APC oncogenic pathways connected with the cell proliferation and inflammation response

361   of hypoxia *(Rosenberger et al. 2009; Zhou et al. 2015)*. GPS2, as a molecular guardian, is

362   necessary for precise control of inflammatory responses involved in immunity and homeostasis

363   *(Cardamone et al. 2012; Venteclef et al. 2010)*. Yeats4, which encodes the YEATS domain

364   containing 4, is closely related to cell proliferation in the cancer process *(Ji et al. 2017; Jixiang*

365   *et al. 2017; Pikor et al. 2013)*. Hivep2, which encodes human immunodeficiency virus type I

366   enhancer-binding protein 2, is associated with developmental delay, intellectual disability, and

367   dysmorphic features *(Steinfeld et al. 2016)*. These 15 genes have the potential to diagnose the

368   extent of wounds and deserve to be explored further.

369   Having identified genes for evaluating the severity of a wound, we next used a time-series

370   analysis based on the "time course" package in R language to find indicators for wound aging in

371   the mild and severe contusion groups, respectively. As a result, the top 60 genes with large

372   differences in temporal patterns among different time points post-injury were acquired for each

373   group based on HotellingT2 values (Table S3-4). There were 30 genes that were shared by the

374   mild and severe injury groups, and their expression profiles were strongly correlated with time in

375 both contusion groups. This indicates that there were similar molecular and cellular responses

376 during the skeletal muscle repair process, although these responses were affected by the severity

377 of the injury. These shared genes were primarily involved in the inflammatory response and in

378 cytokine activity such as Ccr1, Il6, Ccl7, Pdpn, Spp1, Ccl2 and Timp1, which play vital roles in

379 the wound healing process. The expression of Mt2A, one of the 30 shared genes identified, was

380 verified in our previous study *(Fan et al. 2017)*. In this study, the expression patterns of the

381 shared genes (Rrad, Gpnmb, and Timp1) were also examined using qPCR, which were generally

382 similar to microarray data; the results indicated that the data produced via the Affymetrix array

383 were reliable.

384   In the top 60 genes of mild injury, we found that the top 3 categories of biological processes

385 were related to interspecies interaction between organisms, and inflammatory response to an

386 external stimulus. GO categories of cellular components were associated with myofibril,

387 contractile fiber, and sarcomere, and those of molecule functions were relevant to cytokine

388 activity, signaling receptor activator activity, and receptor-ligand activity, suggesting the

389 importance of these genes during mild injury estimation. However, in the top 60 genes of severe

390 injury, the top 3 categories of biological processes were related to defense response, interspecies

391 interaction between organisms, and response to external biotic stimulus. Those of cellular

392 components were associated with the external side of the plasma membrane, and those of

393 molecule functions were relevant to signaling receptor binding, cytokine activity, and signaling

394 receptor activator activity. There were also common pathways in mild and severe injury

395 estimations such as the IL-17 signaling pathway and the Hematopoietic cell lineage, as well as

396 unique pathways in mild injury estimation including cytokine-cytokine receptor interaction and

397 the TNF signaling pathway (Fig.5c,7c). The genes identified in both mild and severe injury were

398 correlated with cell proliferation and the process of inflammation, indicating that time-dependent

399 genes play an important role in repair after injury.

400   This study identified different criteria and methods of biomarker identification for

401 evaluating the extent of wounds and wound age. In order to identify genes to distinguish the

402 extent of the injury, the unique DEGs, which were only significantly changed in the mild or

403 severe damage groups compared with the control groups, were selected to identify the

404 differences between mild and severe contusions. The expression profiles of the fifteen genes

405 selected for evaluating the extent of the damage differed more in mildly and severely contused

406   muscle than they did when evaluating wound age. Conversely, for wound age estimation, our

407   goal was to find genes expressed over time that contained different information at different time

408   points in mild or severe injury. Therefore, the top 60 genes with a large difference in their

409   temporal patterns were screened for wound age estimation in the mild and severe contusion

410   groups, respectively. All these efforts were made to help improve diagnostic accuracy and

411   narrow the margin of error for wound age estimation based on distinguishing the degree of

412   damage.

413   In this study, microarray analyses were performed to characterize the transcriptional

414   expression changes of mildly and severely contused muscle collected at different time points

415   postinjury. After obtaining thousands of DEGs, PCA, LASSO regression, and time-series

416   analyses were used to select the most powerful predictive genes. Finally, fifteen genes for

417   evaluating the extent of wound damage and the top 60 genes for wound age estimation in mild

418   and severe injury were respectively screened. A functional enrichment analysis revealed that

419   these selected genes are actively involved in the muscle repair process and deserve to be

420   addressed and explored further in relation to wound age estimation.

421   **Conclusions**

422   For an accurate assessment of wound age, while considering the effect of wound severity,

423   we carried out a transcriptome-based microarray assay to obtain the expression profiles of wound

424   healing genes following mild and severe muscle contusions. Using statistical and bioinformatics

425   analyses, diagnostic genes were identified for evaluating the extent of wounds and wound age in

426   future studies. However, there are limitations to this study. The sample size for the microarray

427   analysis was small; further research with larger samples is necessary to validate more biomarkers

428   in contused muscle with different degrees of damage.

429   **Data Availability**

430   The microarray data in this study have been uploaded to GEO (accession number: GSE162565).

431

432

433 **References**

434 Bai RF, Lü XJ, E XF, Yu TS, Liu R, and Zhang HD. 2017. Comparison of the Skin and Skeletal
435   Muscle Contusion in Rats Induced by Blunt Force with Different Heights. Journal of forensic
436   medicine 33:1-5. 10.3969/j.issn.1004-5619.2017.01.001

437 Barington K, and Jensen HE. 2016. The impact of force on the timing of bruises evaluated in a
438   porcine model. Journal of forensic and legal medicine 40:61-66. 10.1016/j.jflm.2016.03.005

439 Bindea G, Mlecnik B, Hackl H, Charoentong P, Tosolini M, Kirilovsky A, Fridman WH, Pagès F,
440   Trajanoski Z, and Galon J. 2009. ClueGO: a Cytoscape plug-in to decipher functionally
441   grouped gene ontology and pathway annotation networks. Bioinformatics 25:1091-1093.
442   10.1093/bioinformatics/btp101

443 Cai C, Masumiya H, Weisleder N, Matsuda N, Nishi M, Hwang M, Ko JK, Lin P, Thornton A,
444   Zhao X, Pan Z, Komazaki S, Brotto M, Takeshima H, and Ma J. 2009. MG53 nucleates
445   assembly of cell membrane repair machinery. Nature cell biology11:56-64. 10.1038/ncb1812

446 Cardamone MD, Krones A, Tanasa B, Taylor H, Ricci L, Ohgi KA, Glass CK, Rosenfeld MG,
447   and Perissi V. 2012. A protective strategy against hyperinflammatory responses requiring the
448   nontranscriptional actions of GPS2. Molecular cell 46:91-104. 10.1016/j.molcel.2012.01.025

449 Casse JM, Martrille L, Vignaud JM, and Gauchotte G. 2016. Skin wounds vitality markers in
450   forensic pathology: An updated review. Medicine, science, and the law 56:128-137.
451   10.1177/0025802415590175

452 Chen X, Cheng Z, Zhang S, Werling D, and Wathes D. 2015. Combining Genome Wide
453   Association Studies and Differential Gene Expression Data Analyses Identifies Candidate
454   Genes Affecting Mastitis Caused by Two Different Pathogens in the Dairy Cow. Open
455   Journal of Animal Sciences 5:358-393. doi: 10.4236/ojas.2015.54040.

456 Chin CH, Chen SH, Wu HH, Ho CW, Ko MT, and Lin CY. 2014. cytoHubba: identifying hub
457   objects and sub-networks from complex interactome. BMC systems biology 8 Suppl 4:S11.
458   10.1186/1752-0509-8-s4-s11

459 Dang LH, Feng N, An GS, Cao J, Du QX, Jin QQ, Huang P, and Sun JH. 2020. Novel insights
460   into wound age estimation: combined with "up, no change, or down" system and cosine
461   similarity in python environment. International journal of legal medicine 134:2177-2186.
462   10.1007/s00414-020-02411-z

463 Du QX, Li N, Dang LH, Dong TN, Lu HL, Shi FX, Jin QQ, Jie C, and Sun JH. 2020. Temporal
464   expression of wound healing-related genes inform wound age estimation in rats after a
465   skeletal muscle contusion: a multivariate statistical model analysis. International journal of
466   legal medicine 134:273-282. 10.1007/s00414-018-01990-2

467 Fan HL, Liu SF, Sun JH, and Wang YY. 2017. Time-dependent Expression of MT1A mRNA and
468   MT2A mRNA in the Contused Skeletal Muscle of Rats. Journal of forensic medicine 33:6-
469   10. 10.3969/j.issn.1004-5619.2017.01.002

470 Friedman J, Hastie T, and Tibshirani R. 2010. Regularization Paths for Generalized Linear Models
471   via Coordinate Descent. Journal of statistical software 33:1-22.

472 Grellner W, and Madea B. 2007. Demands on scientific studies: Vitality of wounds and wound

473   age estimation. Forensic Science International 165:150-154. 10.1016/j.forsciint.2006.05.029

474   Hassan Gaballah M, Fukuta M, Maeno Y, Seko-Nakamura Y, Monma-Ohtaki J, Shibata Y, Kato
475   H, Aoki Y, and Takamiya M. 2016. Simultaneous time course analysis of multiple markers
476   based on DNA microarray in incised wound in skeletal muscle for wound aging. Forensic
477   Science International 266:357-368. 10.1016/j.forsciint.2016.06.027

478   Ishida Y, Kuninaka Y, Nosaka M, Kimura A, Kawaguchi T, Hama M, Sakamoto S, Shinozaki K,
479   Eisenmenger W, and Kondo T. 2015. Immunohistochemical analysis on MMP-2 and MMP-
480   9 for wound age determination. International journal of legal medicine 129:1043-1048.
481   10.1007/s00414-015-1167-5

482   Ishida Y, Kuninaka Y, Nosaka M, Shimada E, Hata S, Yamamoto H, Hashizume Y, Kimura A,
483   Furukawa F, and Kondo T. 2018. Forensic application of epidermal AQP3 expression to
484   determination of wound vitality in human compressed neck skin. International journal of legal
485   medicine 132:1375-1380. 10.1007/s00414-018-1780-1

486   Ji S, Zhang Y, and Yang B. 2017. YEATS Domain Containing 4 Promotes Gastric Cancer Cell
487   Proliferation and Mediates Tumor Progression via Activating the Wnt/β-Catenin Signaling
488   Pathway. Oncology research 25:1633-1641. 10.3727/096504017x14878528144150

489   Jixiang C, Shengchun D, Jianguo Q, Zhengfa M, Xin F, Xuqing W, Jianxin Z, and Lei C. 2017.
490   YEATS4 promotes the tumorigenesis of pancreatic cancer by activating beta-catenin/TCF
491   signaling. Oncotarget 8:25200-25210. 10.18632/oncotarget.15633

492   Jung SY, and Ko YG. 2010. TRIM72, a novel negative feedback regulator of myogenesis, is
493   transcriptionally activated by the synergism of MyoD (or myogenin) and MEF2. Biochemical
494   and biophysical research communications 396:238-245. 10.1016/j.bbrc.2010.04.072

495   Ko DC, Gamazon ER, Shukla KP, Pfuetzner RA, Whittington D, Holden TD, Brittnacher MJ,
496   Fong C, Radey M, Ogohara C, Stark AL, Akey JM, Dolan ME, Wurfel MM, and Miller SI.
497   2012. Functional genetic screen of human diversity reveals that a methionine salvage enzyme
498   regulates inflammatory cell death. Proceedings of the National Academy of Sciences of the
499   United States of America 109:E2343-2352. 10.1073/pnas.1206701109

500   Komamura K, Shirotani-Ikejima H, Tatsumi R, Tsujita-Kuroda Y, Kitakaze M, Miyatake K,
501   Sunagawa K, and Miyata T. 2003. Differential gene expression in the rat skeletal and heart
502   muscle in glucocorticoid-induced myopathy: analysis by microarray. Cardiovascular drugs
503   and therapy 17:303-310. 10.1023/a:1027352703783

504   Kubo H, Hayashi T, Ago K, Ago M, Kanekura T, and Ogata M. 2014. Temporal expression of
505   wound healing-related genes in skin burn injury. Legal medicine (Tokyo) 16:8-13.
506   10.1016/j.legalmed.2013.10.002

507   Lee CS, Yi JS, Jung SY, Kim BW, Lee NR, Choo HJ, Jang SY, Han J, Chi SG, Park M, Lee JH,
508   and Ko YG. 2010. TRIM72 negatively regulates myogenesis via targeting insulin receptor
509   substrate-1. Cell death and differentiation 17:1254-1265. 10.1038/cdd.2010.1

510   Li N, Du Q, Bai R, and Sun J. 2018. Vitality and wound-age estimation in forensic pathology:
511   review and future prospects. Forensic Sciences Research 5:15-24.
512   10.1080/20961790.2018.1445441

513 Li Z, Pan J, Ma J, Zhang Z, and Bai Y. 2017. Microarray gene expression of periosteum in
514   spontaneous bone regeneration of mandibular segmental defects. Scientific reports 7:13535.
515   10.1038/s41598-017-13586-8
516 Ling XB, Wei HW, Wang J, Kong YQ, Wu YY, Guo JL, Li TF, and Li JK. 2016. Mammalian
517   Metallothionein-2A and Oxidative Stress. International journal of molecular sciences 17.
518   10.3390/ijms17091483
519 Pikor LA, Lockwood WW, Thu KL, Vucic EA, Chari R, Gazdar AF, Lam S, and Lam WL. 2013.
520   YEATS4 is a novel oncogene amplified in non-small cell lung cancer that regulates the p53
521   pathway. Cancer research 73:7301-7312. 10.1158/0008-5472.can-13-1897
522 Rosenberger P, Schwab JM, Mirakaj V, Masekowsky E, Mager A, Morote-Garcia JC, Unertl K,
523   and Eltzschig HK. 2009. Hypoxia-inducible factor-dependent induction of netrin-1 dampens
524   inflammation caused by hypoxia. Nature immunology 10:195-202. 10.1038/ni.1683
525 Shannon P, Markiel A, Ozier O, Baliga NS, Wang JT, Ramage D, Amin N, Schwikowski B, and
526   Ideker T. 2003. Cytoscape: a software environment for integrated models of biomolecular
527   interaction networks. Genome research 13:2498-2504. 10.1101/gr.1239303
528 Steinfeld H, Cho MT, Retterer K, Person R, Schaefer GB, Danylchuk N, Malik S, Wechsler SB,
529   Wheeler PG, van Gassen KL, Terhal PA, Verhoeven VJ, van Slegtenhorst MA, Monaghan
530   KG, Henderson LB, and Chung WK. 2016. Mutations in HIVEP2 are associated with
531   developmental delay, intellectual disability, and dysmorphic features. Neurogenetics 17:159-
532   164. 10.1007/s10048-016-0479-z
533 Sun JH, Zhu XY, Dong TN, Zhang XH, Liu QQ, Li SQ, and Du QX. 2017. An "up, no change, or
534   down" system: Time-dependent expression of mRNAs in contused skeletal muscle of rats
535   used for wound age estimation. Forensic Science International 272:104-110.
536   10.1016/j.forsciint.2017.01.012
537 Tai YC, and Speed TP. 2009. On gene ranking using replicated microarray time course data.
538   Biometrics 65:40-51. 10.1111/j.1541-0420.2008.01057.x
539 Tibshirani R. 1997. The lasso method for variable selection in the Cox model. Statistics in
540   medicine 16:385-395. 10.1002/(sici)1097-0258(19970228)16:4<385::aid-sim380>3.0.co;2-3
541 Trautz F, Franke H, Bohnert S, Hammer N, Müller W, Stassart R, Tse R, Zwirner J, Dreßler J, and
542   Ondruschka B. 2019. Survival-time dependent increase in neuronal IL-6 and astroglial GFAP
543   expression in fatally injured human brain tissue. Scientific reports 9:11771. 10.1038/s41598-
544   019-48145-w
545 Venteclef N, Jakobsson T, Ehrlund A, Damdimopoulos A, Mikkonen L, Ellis E, Nilsson LM,
546   Parini P, Jänne OA, Gustafsson JA, Steffensen KR, and Treuter E. 2010. GPS2-dependent
547   corepressor/SUMO pathways govern anti-inflammatory actions of LRH-1 and LXRbeta in
548   the hepatic acute phase response. Genes & development 24:381-395. 10.1101/gad.545110
549 Wang L-L, Zhao R, Liu C-S, Liu M, Li S-S, Li J-Y, Jiang S-K, Zhang M, Tian Z-L, Wang M,
550   Zhang M-Z, and Guan D-W. 2016. A fundamental study on the dynamics of multiple
551   biomarkers in mouse excisional wounds for wound age estimation. Journal of forensic and
552   legal medicine 39:138-146. 10.1016/j.jflm.2016.01.027

553 Wang Y, Yamamoto Y, Kuninaka Y, Kondo T, and Furukawa F. 2015. Forensic Potential of
554   MMPs and CC Chemokines for Wound Age Determination. Journal of forensic sciences
555   60:1511-1515. 10.1111/1556-4029.12831
556 Wiese CB, Zhong J, Xu ZQ, Zhang Y, Ramirez Solano MA, Zhu W, Linton MF, Sheng Q, Kon
557   V, and Vickers KC. 2019. Dual inhibition of endothelial miR-92a-3p and miR-489-3p reduces
558   renal   injury-associated   atherosclerosis.   Atherosclerosis   282:121-131.
559   10.1016/j.atherosclerosis.2019.01.023
560 Yan J, Wu L, Jia C, Yu S, Lu Z, Sun Y, and Chen J. 2020. Development of a four-gene prognostic
561   model for pancreatic cancer based on transcriptome dysregulation. Aging (Albany NY)
562   12:3747-3770. 10.18632/aging.102844
563 Zhou Z, Xie J, Cai Y, Yang S, Chen Y, and Wu H. 2015. The significance of NTR1 expression
564   and its correlation with β-catenin and EGFR in gastric cancer. *Diagnostic pathology* 10:128.
565   10.1186/s13000-015-0356-3
566

Figure 1

Fig.1. Flow diagram of the experimental design and data analysis used in the present study.
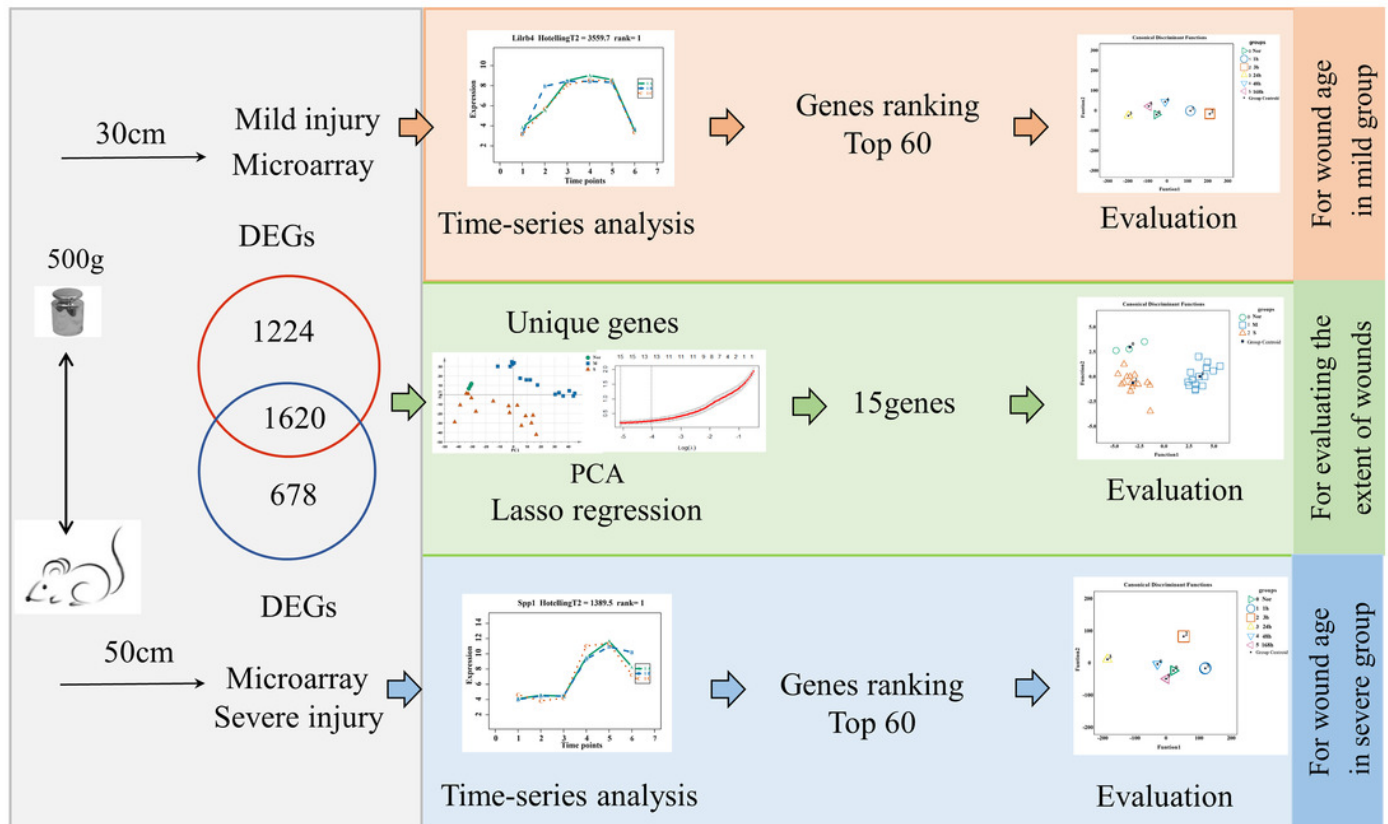
Figure 2

Fig.2. Dynamic transcriptome changes in mildly and severely contused muscle.

(a) The number of DEGs with P<0.05 and 2-fold change at each time point in the mild and severe contusion groups. (b) The number of upregulated and downregulated DEGs in the mild injury groups. (c) The number of upregulated and downregulated DEGs in the severe injury groups. (d) Venn diagram showing that there were 1,620 common genes shared and 1,903 unique genes between the mild and severe contusion groups. (e) The PCA result of unique genes between the mild and severe contusion groups; samples were colored according to the degree of damage. "Nor" means normal groups (in bluish green); "M" means mild injury groups (in blue); "S" means severe injury groups (in vermilion).
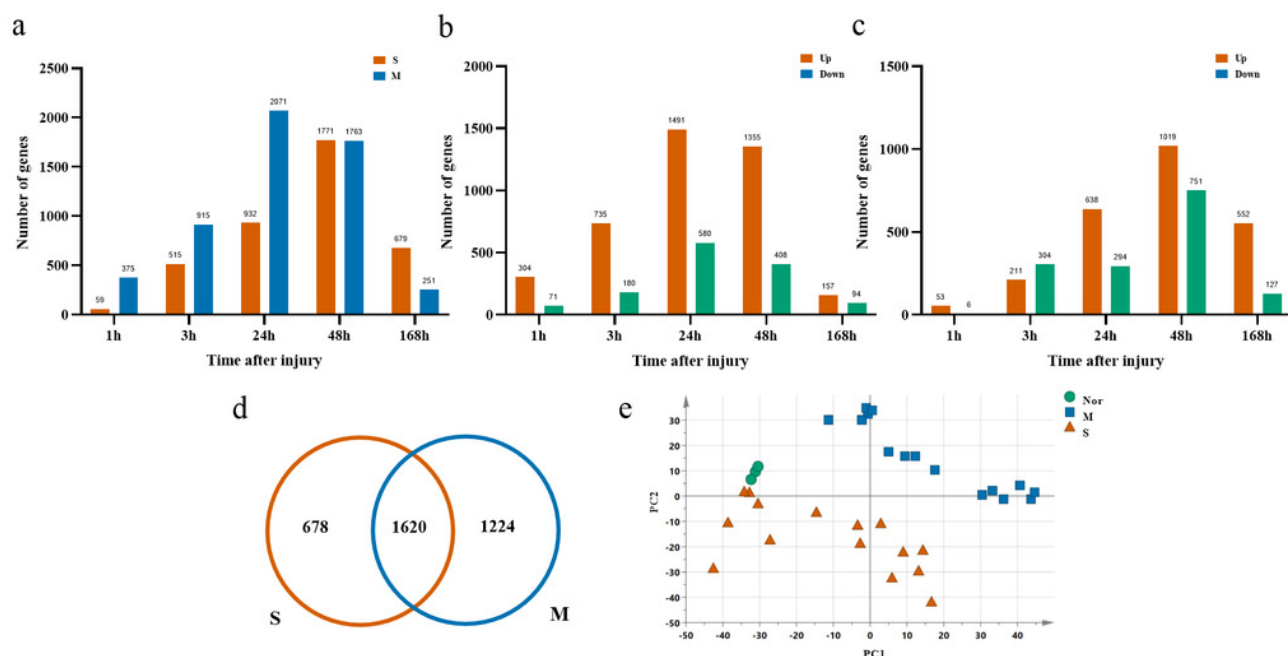
Figure 3

Fig.3. Identification of genes that drive the differences in gene expression between mild and severe injury.

(a) Percentage of variance explained by each principal component. (b-c) The score plots of principal component (PC)1 and PC2. (d-e) PCA (d) and Random Forest (e) of the 15 prognostic DEGs showed that the control group and the mild and severe contusion groups were clearly separated from each other. "Nor" means normal groups (in bluish green); "M" means mild injury groups (in blue); "S" means severe injury groups (in vermilion) .
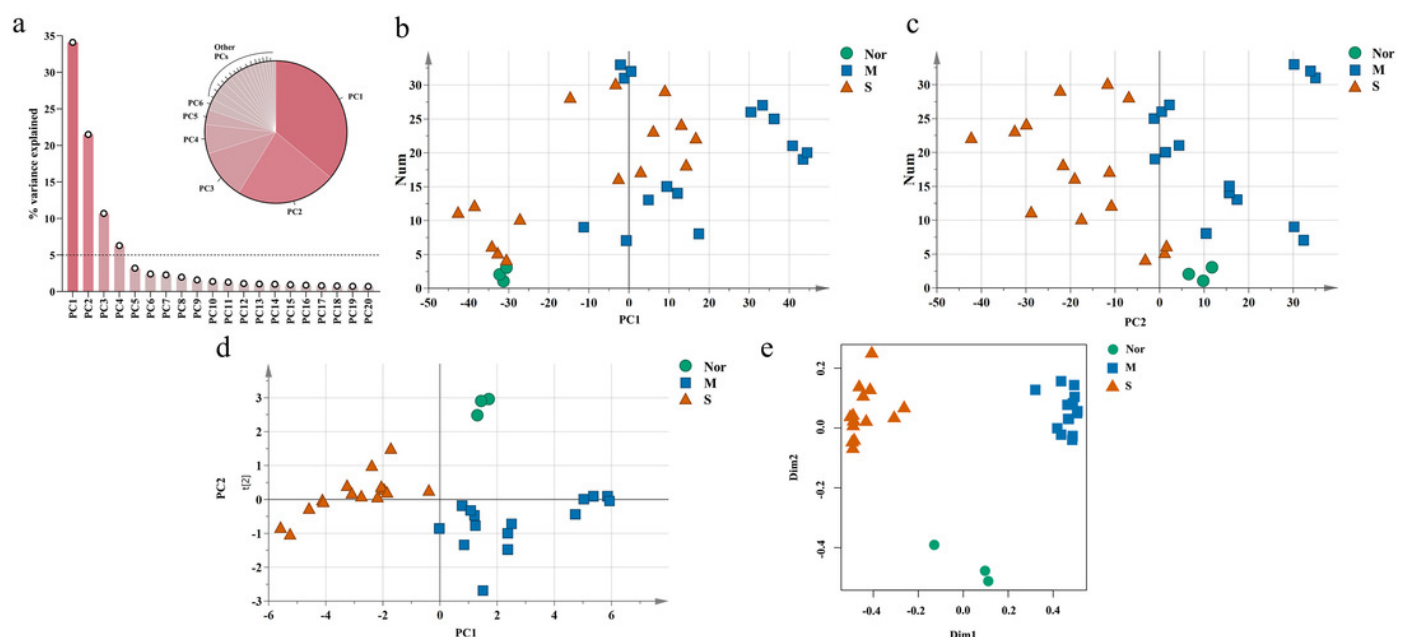
Figure 4

Fig.4. Time-series analysis of differentially expressed genes in mild contusion groups.

(a) Unsupervised hierarchical clustering of gene expression profiles. (b) Principal component analysis of differentially expressed genes in all biological replicates. (c-e) Top 3 significant genes according to HotellingT2 value; 1A (in bluish green), 2B (in blue), and 3C (in vermilion) represent the three biological replicates at each time point. (f) Heatmap of the expression levels of the top 60 differentially expressed genes in the mild injury groups, showing that the expression can be clustered into four temporal patterns. (g) The performance of t-SNE based on these 60 genes.
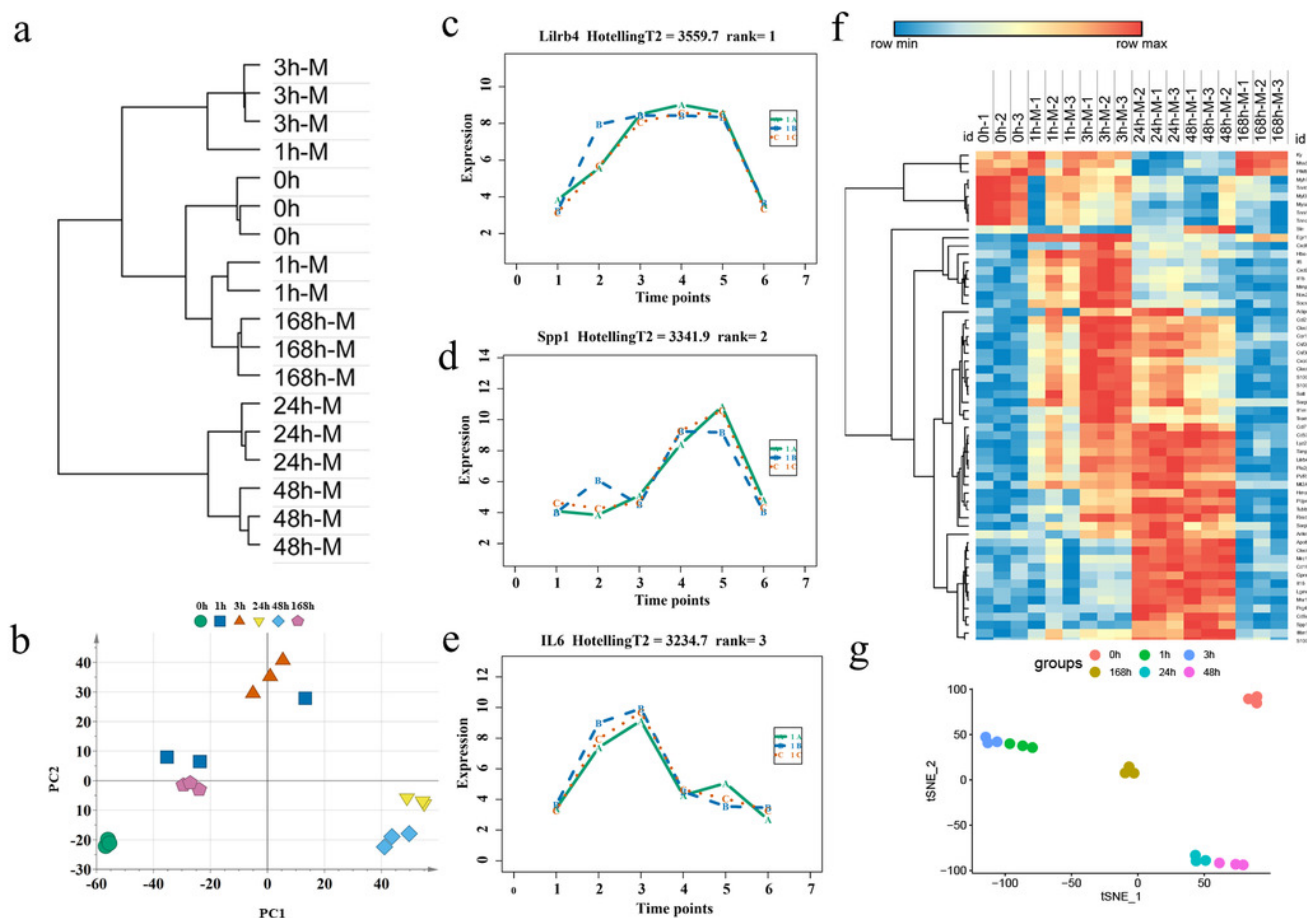
Figure 5

Fig.5. Functional analysis of top 60 differentially expressed genes in mild injury.

(a) Go enrichment; BP, biological progress; CC, cellular component; MF, molecular function.

(b) Kegg analysis using the clueGo plugin in Cytoscape 3.7.2. (c) Functional network of genes. The more reddish the node, the higher the connectivity degree of the node.
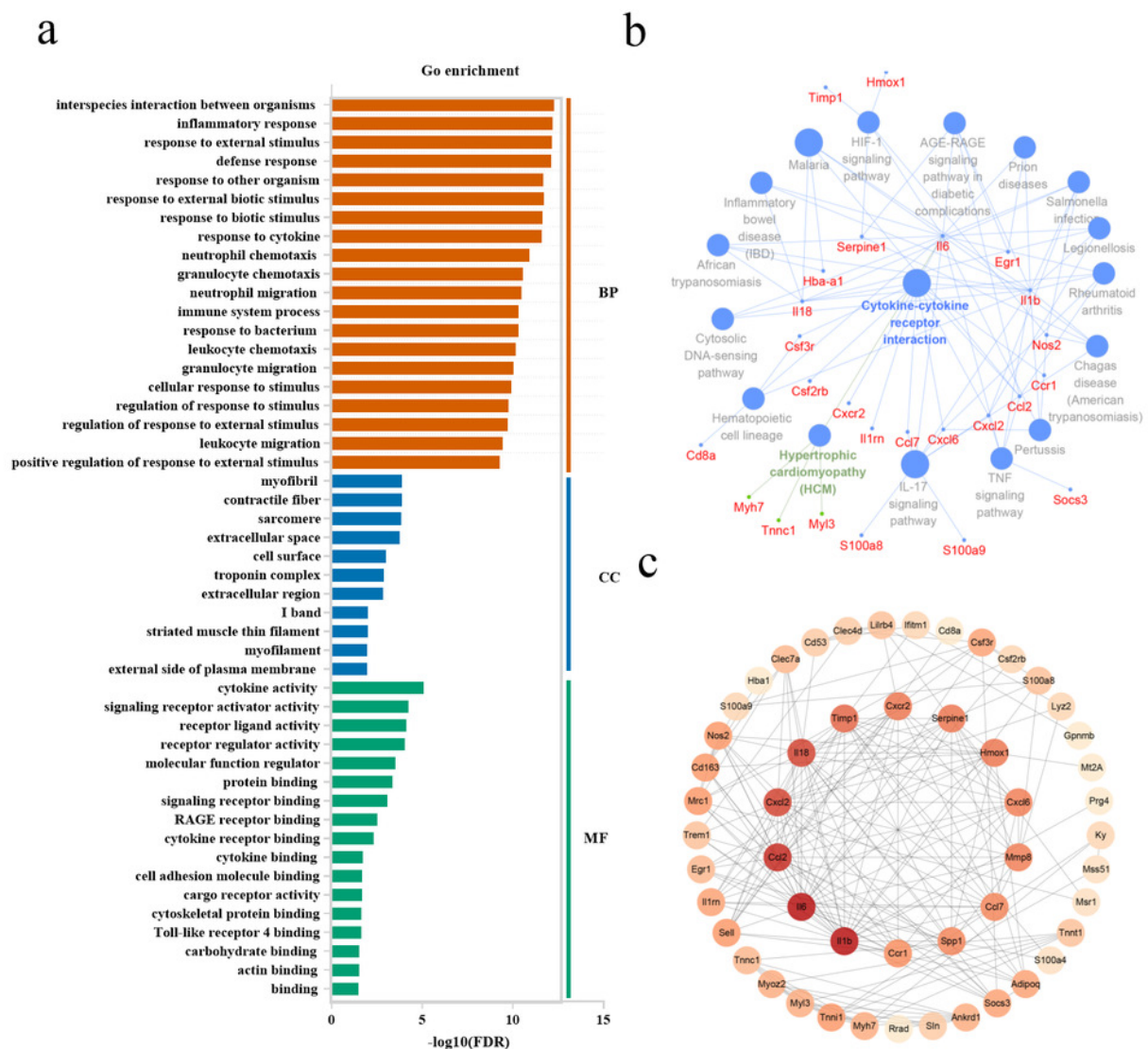
Figure 6

Fig.6. Time-series analysis of differentially expressed genes in severe contusion groups.

(a) Unsupervised hierarchical clustering of gene expression profiles. (b) Principal component analysis of differentially expressed genes in all biological replicates. (c-e) Top 3 significant genes according to HotellingT2 value; 1A (in bluish green), 2B (in blue), and 3C (in vermilion) represent the three biological replicates at each time point. (f) Heatmap of the top 60 differentially expressed genes in the severe injury groups. (g) The t-SNE analysis of these 60 genes in the severe injury group.

Figure 7

Fig.7. Functional and pathway enrichment of differentially expressed genes in severe injury groups.

(a) Go enrichment; BP, biological progress; CC, cellular component; MF, molecular function.

(b) Kegg analysis by clueGo plugin in Cytoscape 3.7.2. (c) Functional network of these genes.

The more reddish the node, the higher the connectivity degree of the node is.
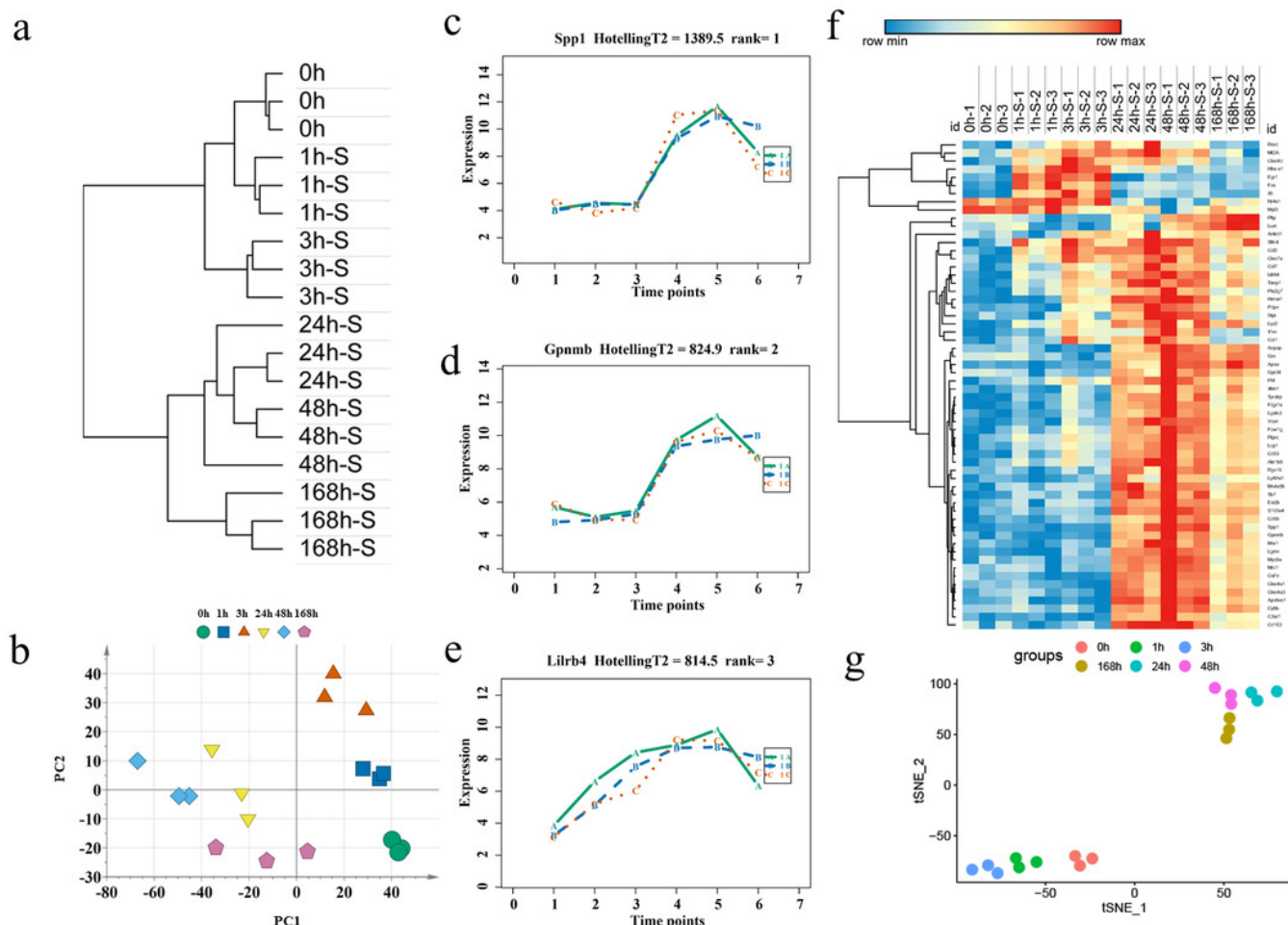
Figure 8

Fig.8. Expression level of Mt2a, Rrad, Gpnmb and Timp1 in microarray analysis (a-d) and RT-qPCR (e-h) in mild group.

a-d 1A (in bluish green), 2B (in blue), and 3C (in vermilion) represent the three biological replicates in microarray analysis .
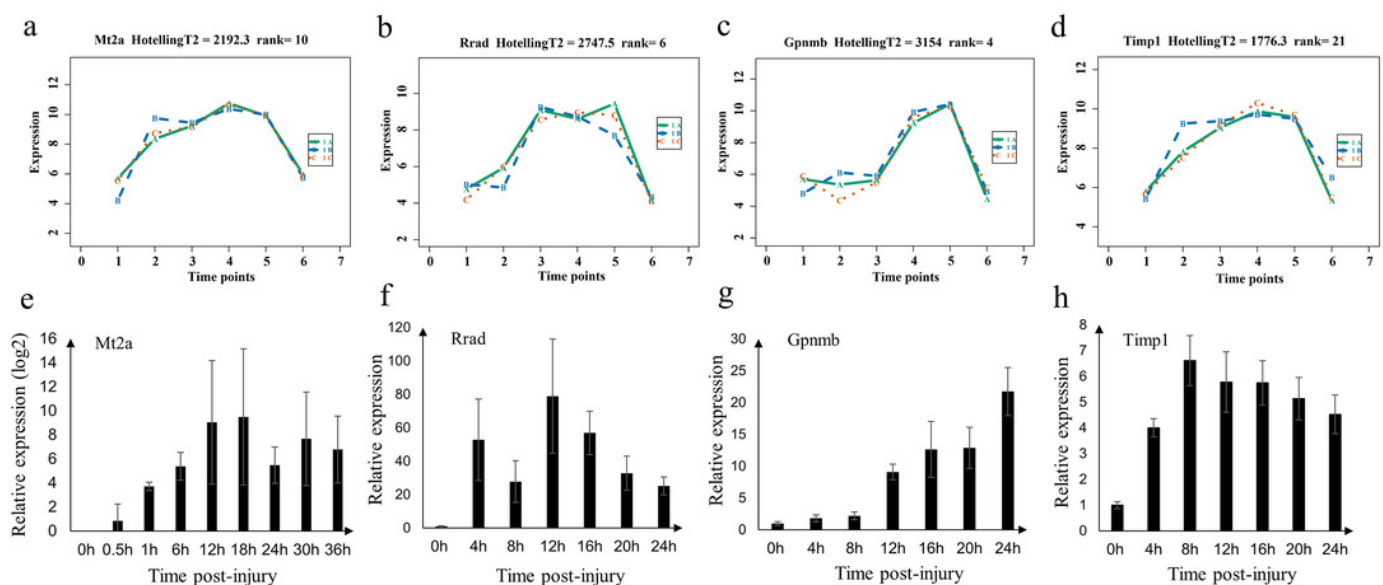
Figure 9

Fig.9. Performance of genes we selected for wound degree and age estimation in Fisher discriminant analysis (FDA) model.

(a) The canonical discrimination functions for the degree of damage. 0◇ control group, 1○ mild injury group, 2□ severe injury group (b, c) The FDA function for wound age estimation in mild and severe injury groups. The Wilks' lambda option was used in the Stepwise method. (0 ▷ 0h, 1○ 1h, 2□ 3h, 3△ 24h ,4▽ 48h, 5◁ 168h).